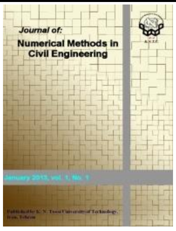

Numerical Methods in Civil Engineering

Real-time damage detection of bridges using adaptive time-frequency analysis and ANN

Vahid Ahmadian*, Seyed Bahram Beheshti Aval, Ehsan Darvishan*****

ARTICLE INFO

Article history:
Received:
May 2019.
Revised:
July 2019.
Accepted:
August 2019.

Keywords:
Bridge health monitoring
Damage detection
Hilbert–Huang Transform
Artificial Neural Network
Signal processing

Abstract:

Although traditional signal-based structural health monitoring algorithms have been successfully employed for small structures, their application for large and complex bridges has been challenging due to non-stationary signal characteristics with a high level of noise. In this paper, a promising damage detection algorithm is proposed by incorporation of adaptive signal processing and Artificial Neural Network (ANN). First, three adaptive signal processing techniques including Empirical Mode Decomposition (EMD), Local Mean Decomposition (LMD) and Hilbert Vibration Decomposition (HVD) are compared. The efficacy of these methods is examined for several numerically simulated signals to find a reliable signal processing tool. Then, three signal features are compared to find the most sensitive feature to damage. In the next step, an ANN ensemble is utilized as a classifier. Traditional statistical features and energy indices are used as the network input and output to make real-time detection of damage possible. The strength of this approach lies with training the network only based on healthy state of the structure. Having a trained ANN, online processing can be made to find a possible damage. Results show that the proposed algorithm has a good capacity as an online output-only damage detection method.

1. Introduction

Structural health monitoring has always been a primary concern to ensure serviceability and safety of vital infrastructures like bridges. In the past few decades, signal-based damage detection methods have become a hot area, especially for large and complex structures [1]. In this context, a majority of the research efforts have been devoted to traditional signal processing techniques such as Fourier and wavelet transforms [2]. However, these methods use a pre-defined shape function which reduces their instantaneous properties and yield low frequency resolution [3].

* *MSc., Department of Civil Engineering, K. N. Toosi University of Technology, Tehran, Iran.*
** *Corresponding Author: Associate Professor, Department of Civil Engineering, K. N. Toosi University of Technology, Tehran, Iran Email: beheshti@kntu.ac.ir*
*** *Assistant Professor, Department of Civil Engineering, Roudehen Branch, Islamic Azad University, Roudehen, Iran*

Since changes due to damage in complex structures is not very large, using signal processing procedures with high frequency resolution can help improve the ability of the damage detection methods to differentiate healthy and damaged states. Recently, adaptive signal processing methods have attracted increasing attention since they can capture nonlinear and nonstationary signals (real world signals) [4].

Zhang et al. [5] compared Fourier and Hilbert–Huang transform (HHT) [6] based on dynamic response of Trinity River Relief Bridge. They claimed that frequency downshift is an indication of damage extent. Liu et al. [7] could detect and locate damage in an actual benchmark data. They compared empirical mode decomposition (EMD) and wavelet analysis, and concluded that EMD has a better denoising capability than wavelet. By using a combination of EMD and wavelet analysis, Li et al. [8] could identify the location and severity of damage. Dong et al. [9] proposed a damage index by utilizing EMD and vector autoregressive moving average (VARMA) model.

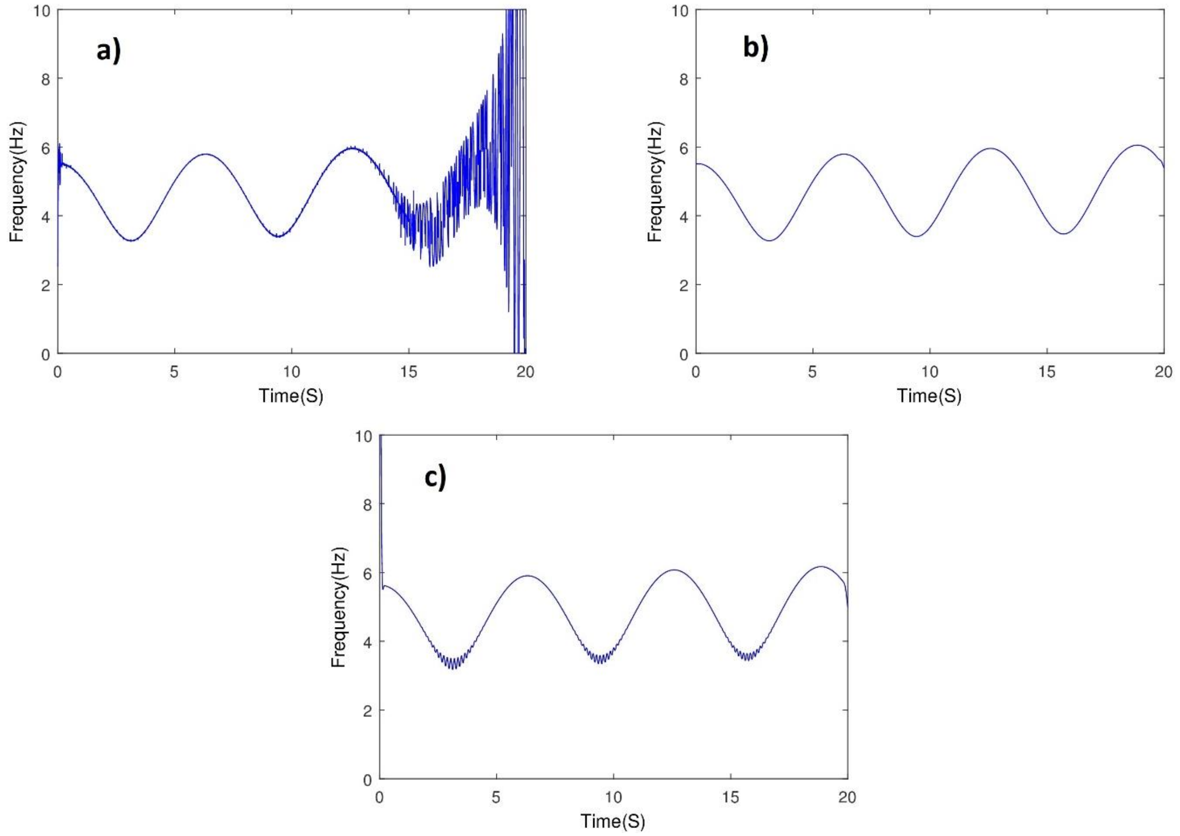

Fig. 1: Instantaneous Frequency of SDOF System a) EMD b) LMD c**)** HVD

They used two real benchmark structures to verify their damage detection method in real conditions. Liu et al. [10] established a HHT managing system to monitor aging process in Taiwan bridges. They analyzed ambient vibration of bridges to investigate changes in structural properties due to environmental conditions. Roveri and Carcaterra [11] proposed a HHT-based damage detection technique for bridges under traveling load. They conducted theoretical and numerical studies to identify the capability of their method. Kuwar et al. [12] used wireless sensors to study damage occurrence in a single span bridge under passing vehicles. They used marginal Hilbert spectrum to identify three pre-defined damage cases. Hsu et al. [13] proposed two damage indices based on HHT including the ratio of bandwidth (RB) and the ratio of effective stiffness (RES). They tested the algorithm on MDOF structures with various frequencies. Ramezani and Bahar [14] used EMD to find mode shapes of a structure. Their method was an output only procedure and was verified with two case studies. One an analytical model and the other the UCLA factor building. Wang and Chan [15] summarized existing methods for condition assessment of bridges. They conducted a review on vibration-based methods with the focus on statistical methods and signal processing techniques. A comprehensive review on application of HHT in structural health monitoring was carried out by Chen et al. [16].

Although HHT is successfully implemented in several damage detection algorithms, it suffers from several shortcomings [17]. Several adaptive signal processing methods are proposed to solve the HHT problems. Among these methods, Local Mean Decomposition (LMD) [18] and Hilbert Vibration Decomposition (HVD) [19] are not utilized for bridge health monitoring. Also, HHT is computer-intensive [20] and is not applicable for online monitoring. On this basis, the present paper has focused on presenting a promising methodology for online health monitoring of bridges subjected to traffic loading. To this end, the paper is organized into two parts. Several instantaneous signal processing techniques are compared in the first part to find a reliable signal processing tool. Among these procedures, EMD is more conventional. LMD and HVD are more recent and are claimed to outperform EMD in some cases [21,22]. The second part presents an online damage detection approach for the Yonghe bridge as a case study large structure. By application of HHT on sensor acceleration outputs, three signal features are extracted and compared. Energy index of the extracted IMFs is defined as a damage index. Finally, a neural network ensemble is employed to classify damage only based on the statistical parameters of sensor outputs. Using an ensemble of independent networks helps to separate input spaces and reduces the generalization errors. Moreover, neural network ensemble has faster learning ability and needs less computation efforts compared to conventional neural networks used for structural health monitoring.

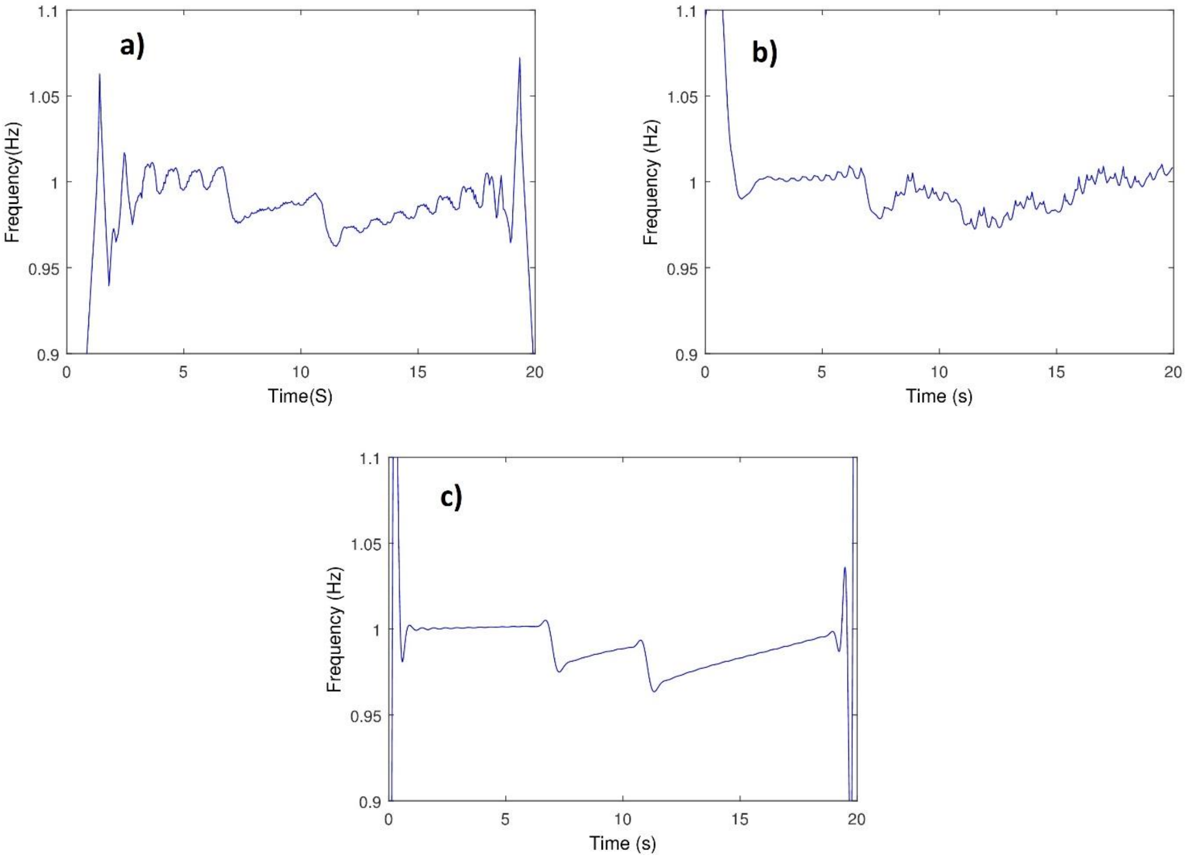

Fig. 2: Instantaneous Frequency of a SDOF System with Stiffness Reduction a**)** EMD b) LMD c) HVD

2. Signal processing procedures

2.1. Hilbert transform

Hilbert transform of a signal, x(t), is a linear operator which refers to the Cauchy principal value (Huang et al., 1998 [6])

$$H[x(t)] = y(t) = \frac{1}{\pi} PV \int_{-\infty}^{+\infty} \frac{x(t)}{t-\tau} d\tau \qquad (1)$$

Where, PV is Cauchy principle value of integral. More details on how to calculate PV is provided by Henrici (1988) [23].

By extension of the signal into complex plane, analytical signal can be defined as:

$$z(t) = x(t) + iy(t) = a(t)e^{i\theta(t)} \qquad (2)$$

Thus,

$$a(t) = \sqrt{x^2(t) + y^2(t)}$$
$$\phi(t) = \arctan(\frac{y}{x}) \qquad (3)$$

Where $a(t)$ is the instantaneous amplitude and $\phi(t)$ is the instantaneous phase. Instantaneous frequency is the time derivative of the phase function.

$$f(t) = \frac{1}{2\pi} \frac{d\phi(t)}{dt} \qquad (4)$$

2.2. Empirical Mode Decomposition (EMD)

Hilbert-Huang transform (HHT) was proposed by Huang et al. (1998) [6], based on a combination of empirical mode decomposition (EMD) and Hilbert transform, for analyzing non-linear and non-stationary signals. The essence of EMD is to employ a sifting process to decompose a multi-component signal into several mono-component functions (IMFs) with variable amplitude and frequency along the time to gain a well-behaved Hilbert transform. Each IMF represents a single oscillation (mono-component). But, unlike the traditional signal processing techniques, IMFs are more general and have variable amplitude and frequency along the time. The decomposition process is as follows:

1. Find local maxima of the signal. Use a spline fitting for the maximum points, $e_u(t)$, to construct an upper envelope.
2. Repeat step (1) for minimum points to find $e_l(t)$. Then, compute the mean of both envelopes, $m_1(t)$.

$$m_1(t) = \frac{e_u(t) + e_l(t)}{2} \qquad (5)$$

3. Subtract the mean function, $m_1(t)$, from the original signal, $x(t)$, to find the first component, $h_1(t)$.

$$h_1(t) = x(t) - m_1(t) \qquad (6)$$

4. Repeat steps (1) to (3) by assuming the first component, $h_1(t)$, as the original signal, $x(t)$. Again, repeat the sifting process k times until the basic conditions are met.

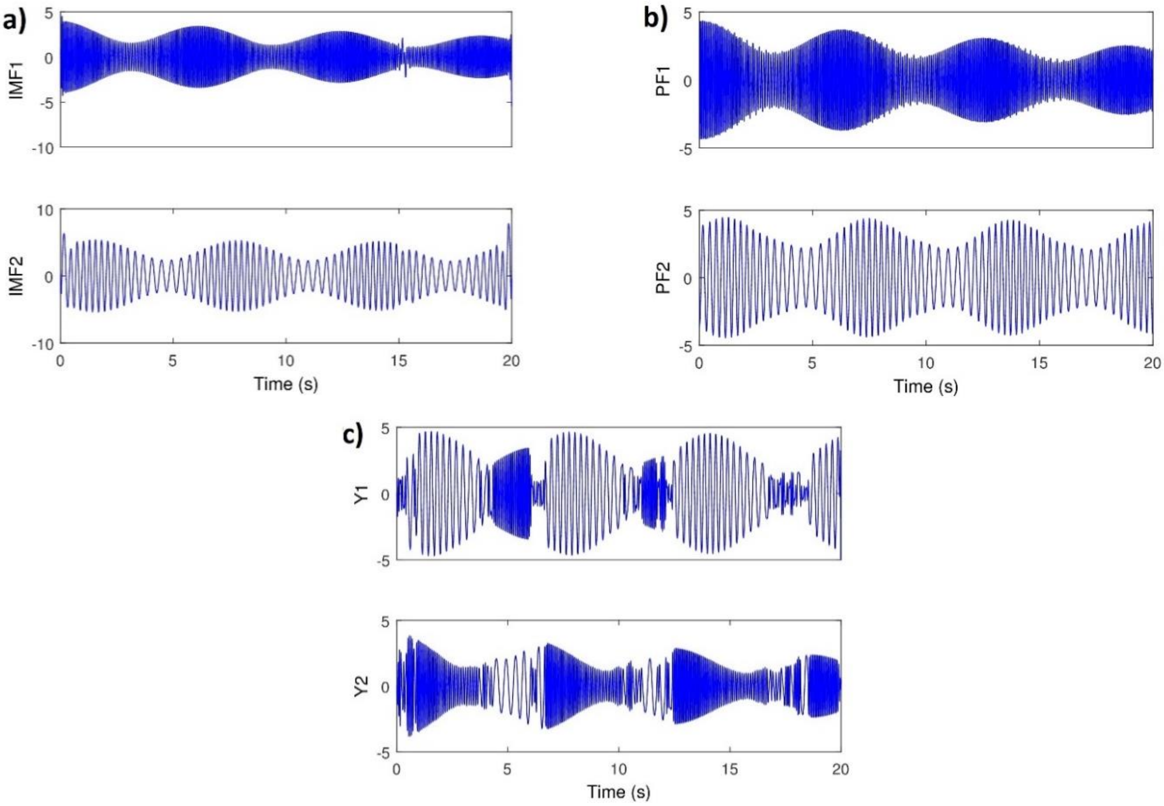

Fig. 3: Vibration Components of a MDOF System a) EMD b) LMD c) HVD

$$h_{1k}(t) = h_{1(k-1)}(t) - m_1 k(t) \tag{7}$$

Consider $h_{1k}(t)$ as the first true IMF.

$$c = h_{1k}(t) \tag{8}$$

5. Huang et al. suggested control of a stopping criterion at each iteration.

$$SD = \sum_{t=0}^{T} \left[\frac{\left| h_{(k-1)}(t) - h_{(k)}(t) \right|^2}{h^2_{(k-1)}(t)} \right] \tag{9}$$

6. Now, subtract the first IMF, c_1, from the signal and consider r_1 as a new signal. Repeat steps (1) to (6) to obtain other IMFs.

$$r_1 = x(t) - c_1 \tag{10}$$

7. The original signal can be reconstructed by superposition of IMFs and the final residue.

$$x(t) = \sum_{j=1}^{n} c_j + r_n \tag{11}$$

2.3. Local Mean Decomposition (LMD)

Local mean decomposition (LMD) is an iterative demodulation technique that is recently developed for the analysis of time-varying signals. Inspired by EMD, it separates a frequency modulated signal from an amplitude modulated envelope signal. The process is briefly described as follows (Smith, 2005 [18]):

1. Calculate the local mean, $m_{ij}(t)$, and local magnitude, $a_{ij}(t)$, from the successive exterma, $n_{ij}(k_l)$, $k_l=k_1,k_2, \ldots,k_M$,

$$m_{ij}(t) = \frac{n_{ij}(k_l) + n_{ij}(k_{l+1})}{2} \qquad k_l = k_1, \ldots, k_{M-1}, \quad t \in [k_l, k_{l+1}) \tag{12}$$

$$a_{ij}(t) = \frac{\left| n_{ij}(k_l) - n_{ij}(k_{l+1}) \right|}{2} \qquad k_l = k_1, \ldots, k_{M-1}, \quad t \in [k_l, k_{l+1}) \tag{13}$$

Where k_l is the order of product function (PF), M is the number of extrema, the subscript i denotes the number of PF and the subscript j denotes the number of iterations needed in a process of PF

2. Use a moving average filter to smooth interpolated local mean $\tilde{m}_{ij}(t)$ and amplitude $\tilde{a}_{ij}(t)$ functions.

3. By definition of $h_{11}(t) = x(t) - \tilde{m}_{11}(t)$ and $s_{11}(t) = \left(h_{11}(t) / \tilde{a}_{11}(t) \right)$, check whether $s_{11}(t)$ is a normalized frequency-modulated signal. If $s_{11}(t)$ is close to 1, go to step (4), otherwise repeat steps (1) and (2) to reach a purely flat FM signal.

4. Instantaneous amplitude, $a_1(t)$, is obtained by multiplication of all $\tilde{a}_{1i}(t)$

$$a_1(t) = \prod \tilde{a}_{1i}(t) \tag{14}$$

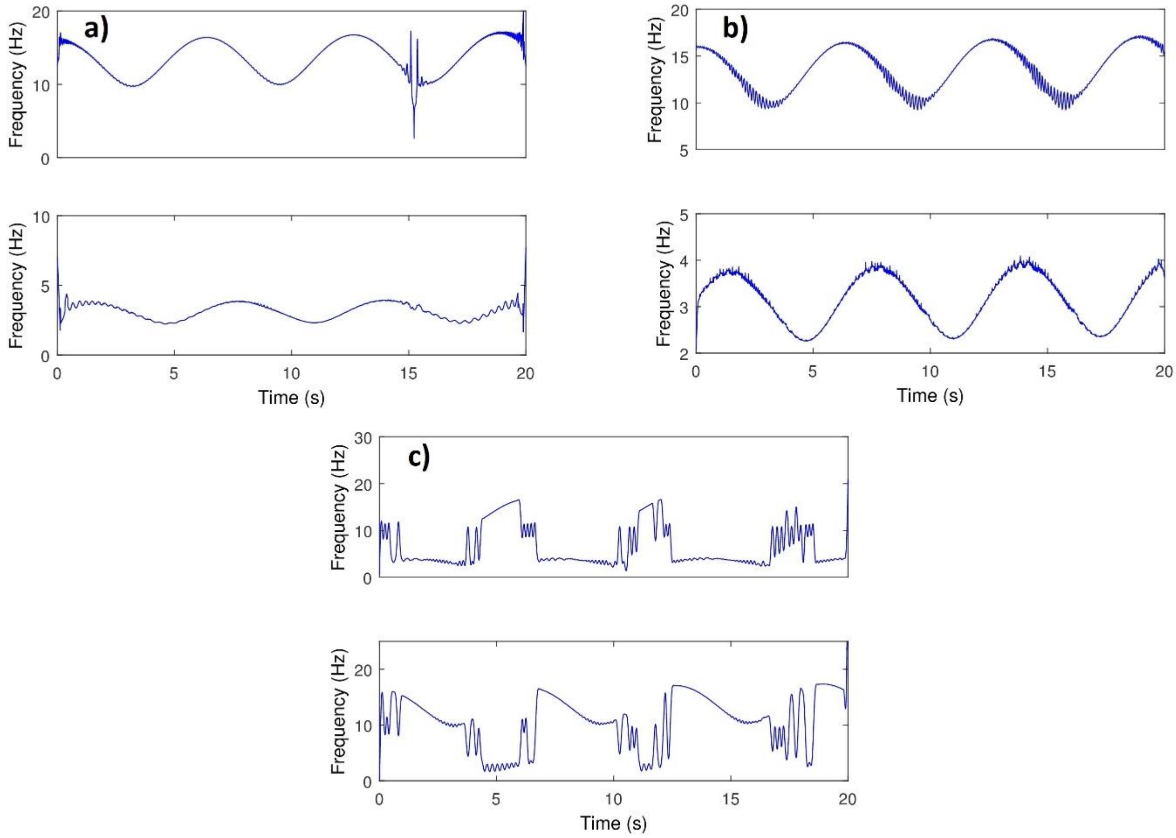

Fig. 4: Instantaneous Frequencies of MDOF System a) EMD b) LMD c) HVD.

5. The instantaneous phase, $\varphi_1(t)$, and the instantaneous frequency, $f_1(t)$, are calculated by:

$$\varphi_1(t) = \arccos\left(s_{1r_1}(t)\right) \tag{15}$$

$$f_1(t) = \frac{f_s d\varphi_1(t)}{2\pi dt} \tag{16}$$

6. By the multiplication of envelope function, $a_1(t)$, and the final frequency demodulated signal, $s_{1r_1}(t)$ the first PF is obtained by:

$$PF_1(t) = a_1(t) s_{1r_1}(t) \tag{17}$$

7. By subtracting, $PF_1(t)$, from the original signal, $x(t)$, smoothed data is obtained which is treated as a new signal.

$$u_1(t) = x(t) - PF_1(t) \tag{18}$$

8. Steps (1) to (4) are repeated until $u_i(t) = u_{i-1}(t) - PF(t)$ becomes a monotonic function. The original signal can be reconstructed by:

$$x(t) = \sum_{i=1}^{p} PF_i(t) + u_p(t) \tag{19}$$

2.4. Hilbert Vibration Decomposition (HVD)

HVD method is an iterative time-varying vibration decomposition technique that is developed for non-stationary wideband vibrations. Unlike the EMD, HVD is directly based on Hilbert transform. Therefore, it does not require any additional signal processing. The main idea of the procedure is described below (Feldman, 2006 [19]):

Assume a simple two-component signal in its analytic form

$$z(t) = a_1(t) e^{i\int_0^t \omega_1(t)dt} + a_2(t) e^{i\int_0^t \omega_2(t)dt} = a(t) e^{i\int_0^t \omega(t)dt} \tag{20}$$

The instantaneous frequencies and amplitudes of the signal are

$$a(t) = \left[a_1^2 + a_2^2 + 2a_1 a_2 \cos\left(\int(\omega_2 - \omega_1)dt\right)\right]^{1/2}$$

$$\omega(t) = \omega_1 + \frac{(\omega_1 - \omega_2)\left[a_2^2 + 2a_1 a_2 \cos\left(\int(\omega_2 - \omega_1)dt\right)\right]}{a^2(t)} \tag{21}$$

The amplitude, $a(t)$, is composed of a slow varying (sum of squared amplitudes of both components) and rapidly varying (oscillating) part. Similarly, the instantaneous frequency, $\omega(t)$, consists of a slowly varying (ω_1) part and a rapidly varying part with asymmetrical oscillation.. If the derivative of a_1 and a_2 is insignificant, assuming $a_1 > a_2$ we get

$$\int_0^T \frac{(\omega_1 - \omega_2)\left[a_2^2 + 2a_1 a_2 \cos\left(\int(\omega_2 - \omega_1)dt\right)\right]}{a^2(t)} = 0 \tag{22}$$

Based on this interesting characteristic, the asymmetrical oscillation can be eliminated using a low-pass filter on the components to extract the largest frequency component.

Fig. 5: Two Views of the Yonghe Bridge

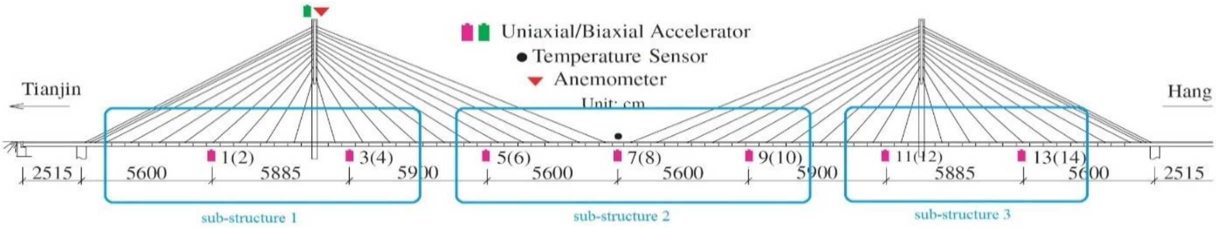

Fig. 6: Sensor Locations of the Health Monitoring System and Location of Substructures

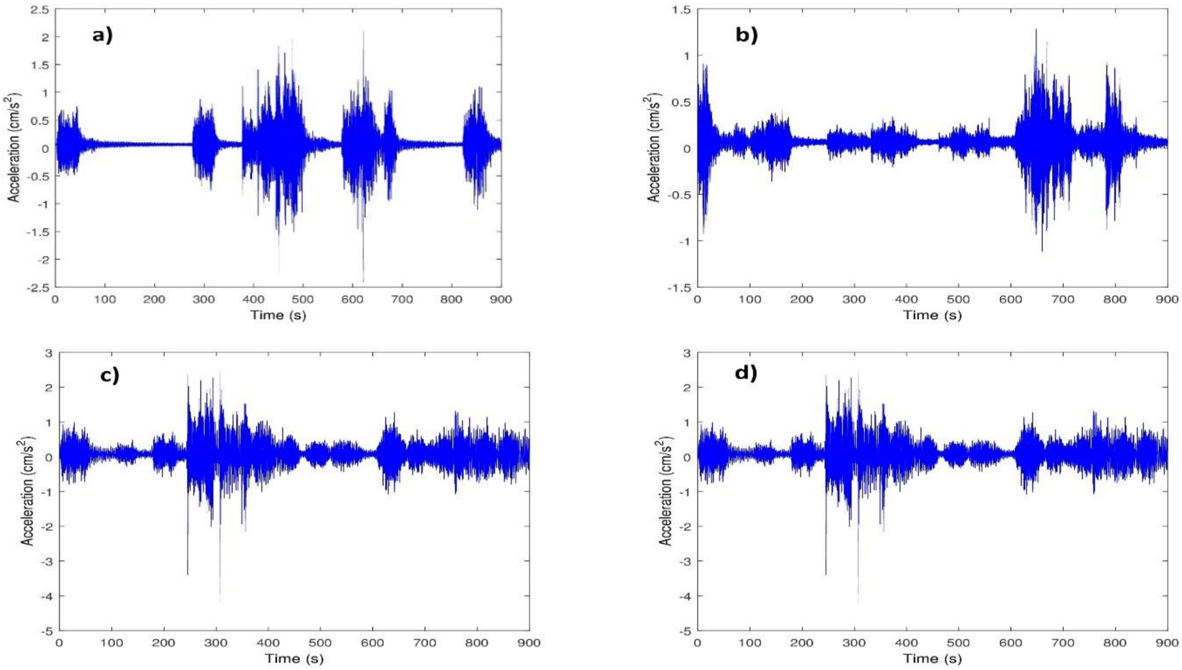

Fig. 7: Acceleration record of sensor 7. (a) Jan, 2008, 5:30 am to 5:45 am; (b) Jan, 2008 12 pm to 12:15 pm; (c) July, 2008, 5:30 am to 5:45 am; (d) July, 2008 12 pm to 12:15 pm

The above property can be extended for multi component signals. Therefore, low-pass filtering is still valid for extraction of largest frequency component. In the next step, HVD uses the well-known synchronous detection technique to find the envelope of the largest energy component. Synchronous detection is a tool that can extract amplitude details about a frequency component when the frequency is known a priori. In summary, the procedure can be summarized as follows:

1. Calculate the analytic form, $z(t)$ of the signal, $x(t)$ by Hilbert transform.

2. Extract the instantaneous frequency using the analytic signal.

3. Eliminate lower vibration components by using a high-pass filter.

4. Calculate the larger amplitude component by synchronous demodulation of the component in step (3).

5. Subtract signal of step (4) from the original signal and repeat steps (1) to (4) until no more extractions are possible.

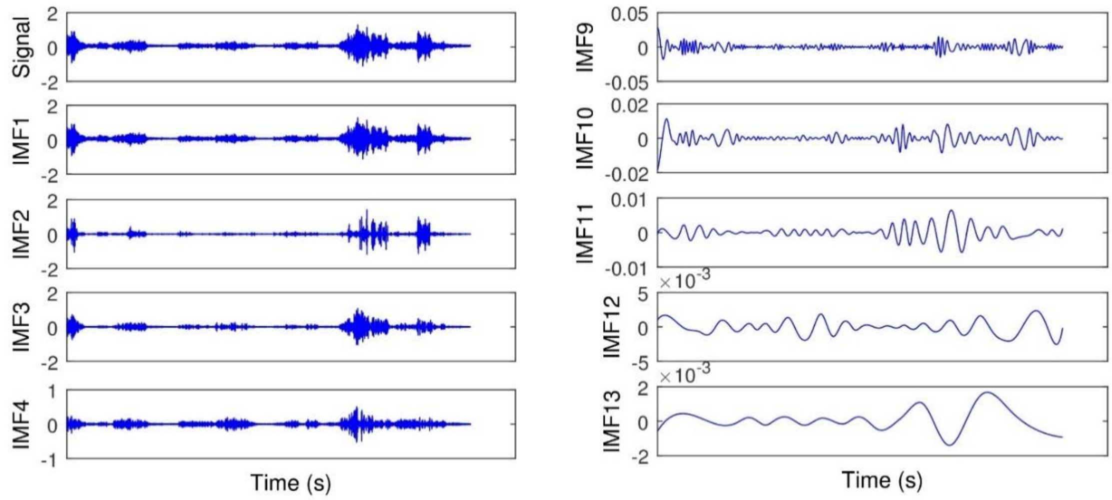

Fig. 8: EMD Results for Healthy State

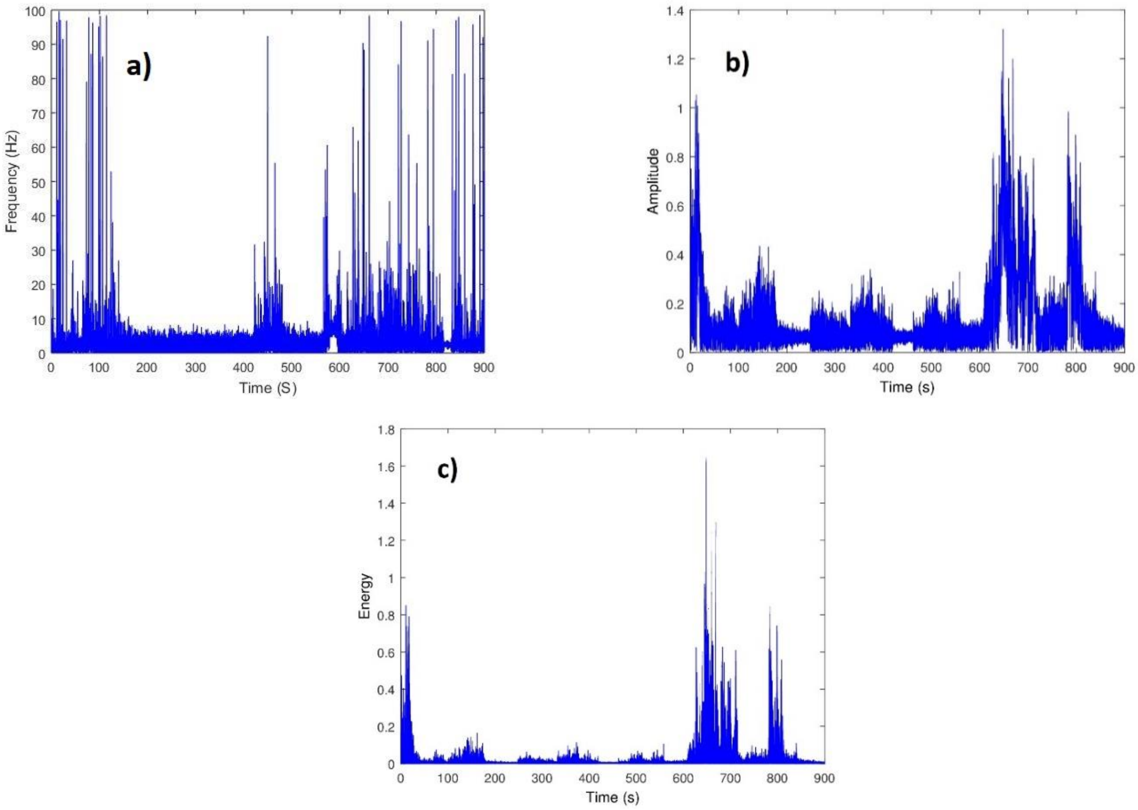

Fig. 9: Instantaneous Functions a) Frequency b) Amplitude c) Energy

3. Comparison of the triple signal processing methods

Since vibration signals of large and complex structures are complicated and are affected by environmental conditions (noise, temperature, and humidity), signal processing method plays a central role to appropriately extract meaningful signal features. On this basis, a comparison is carried out aiming to investigate the sufficiency of the aforementioned signal processing methods. These approaches are applied to nonstationary signals produced by several numerical simulations. They are including two-SDOF and one-MDOF systems with time-varying parameters.

3.1. Slow varying SDOF system

First, a free-vibrating SDOF system of Eq. (23) is selected. Eq. (24) shows the definition of varying mass, stiffness, and damping. Initial velocity of 10 mm/s is defined as the initial condition. The differential equation of motion is solved in 0.001 s time steps using 4th order Runge-Kutta method.

$$m(t)\ddot{x}+c(t)\dot{x}+k(t)x=0 \tag{23}$$

$$\begin{aligned} m(t) &= \left(2+0.5e^{-0.1t}\right)\times 10^3\ kg, \\ k(t) &= \left(2+\cos(t)\right)\times 10^6\ N/m, \\ c(t) &= \left(1+0.25\sin(t)\right)\times 10^3\ N.s/m. \end{aligned} \tag{24}$$

Fig. 1 compares the oscillation frequency of the system obtained by the aforementioned procedures. It is obvious that EMD suffers from end effect problem in which vibration distortion occurs in endpoints. However, several effective tools exist to mitigate end effect problem of EMD. HVD slightly represents unwanted oscillations in crest points which is the consequence of the inability of the procedure to extract pure largest oscillation. In general, all the procedures represent excellent resolution, regardless of end effect problem in EMD.

3.2. SDOF system with sudden stiffness reduction

A SDOF systems is considered with two successive reductions in stiffness at t=7 s and t=11 s (Eq. 25). A harmonic force is applied to the system to model forced vibration of a non-stationary system. Fig. 2 compares the accuracy of the procedures to reveal time instances that stiffness reductions occur. All procedures have tracked sudden changes at t=7 and t=11 seconds. Again, end effect problem is more tangible in EMD. However, EMD has traced sudden frequency changes with acceptable accuracy. LMD shows slightly deviated oscillations. Therefore, frequency jumps are not clear in comparison to EMD and HVD. HVD exhibits a smoother frequency by taking advantage of a low-pass filter in sifting process which eliminates other oscillation amplitudes.

$$\begin{aligned} & m\ddot{u}+c\dot{u}+rk(u+\alpha u^3)= \\ & m[\ddot{u}+2\zeta\omega\dot{u}+r\omega^2(u+\alpha u^3)]=F_0\cos\Omega t, \\ & r=\begin{cases} 0.975-0.025\tanh\dfrac{t-7}{t_r} & for\, 0<t\le 9 \\ 0.925-0.025\tanh\dfrac{t-11}{t_r} & for\, t>9 \end{cases}, \\ & \omega=2\pi,\ \zeta=0.03,\ \alpha=0.1,\ F_0=2, \\ & \Omega=\omega,\ t_r=0.05. \end{aligned} \tag{25}$$

3.3. MDOF systems

A lumped mass 2DOF system is utilized to illustrate the decomposition ability of the procedures. According to Eq. (26), mass, stiffness and damping of this system for any degrees of freedom is assigned. $\{X(0)\}=\{10\quad 0\quad 10\quad 0\}$ is assumed as the initial condition,

$$\begin{aligned} & m_1=m_2=2+0.5e^{-0.05t}\,kg \\ & k_1=(2+\sin(t))\times 10^6\ N/m \\ & k_2=4\times(2+\cos(t))\times 10^6\ N/m \\ & c_1=0.1\times(1+0.5\sin t)\times 10^3\ N.s/m \\ & c_2=0.05\times(1+0.5\cos t)\times 10^3\ N.s/m \end{aligned} \tag{26}$$

Fig. 3 illustrates vibration components of the second DOF. It is clear that EMD and LMD have elaborately demodulated vibration modes. In turn, HVD represents similar scales residing in opposite components due to signal intermittency. In other words, mode mixing problem has resulted in incorporation of second mode of vibration into the first component. Therefore, no meaningful oscillations could be extracted.

Fig. 4 also shows instantaneous frequencies. As expected, EMD and LMD show similar time-frequency representations. However, LMD shows slight noise-like oscillations in both vibration modes. Also, HVD failed to decompose the signal correctly as a result of mode mixing problem.

In brief, both EMD and LMD represent acceptable demodulation capacity. EMD suffers from end effect problem. Instead, LMD could not clearly track sudden frequency changes, although it excels EMD in slow-varying cases. HVD performed well in SDOF cases. However, it yielded poor results in MDOF case making it an unreliable method for this study. Based on the above results, EMD outperformed LMD since several remedies exist to eliminate end effects. Therefore, EMD is selected as a more reliable signal processing tool for the proposed damage detection technique.

4. Structural health monitoring benchmark study

Tianjin Yonghe bridge is a cable-stayed bridge with semi-fan system constructed over the Yongding River in mainland China. It connects Tianjin city to Hangu. The bridge was put into operation at the end of 1987 (Fig. 5). The total length of the bridge is 510.0 m including a 260 m double tower main span and two 25.15 m side spans. A more detailed overview of the bridge can be found in Li et al. (2014) [24] and Kaloop (2010) [25]. The bridge experienced serious damages during its 20 years of operation. In 2005, cracks were observed at the main girder mid-span which were repaired during 2005-2007. Meanwhile, a health monitoring system was installed on the bridge by the Center of SMC at the Harbin Institute of Technology to improve bridge maintenance and to ensure safe operation (Li et al., 2014 [24]).

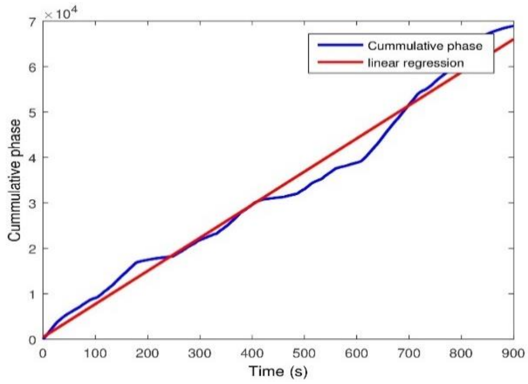

Fig. 10: Cumulative Summation of Absolute Phase Function and Linear Regression

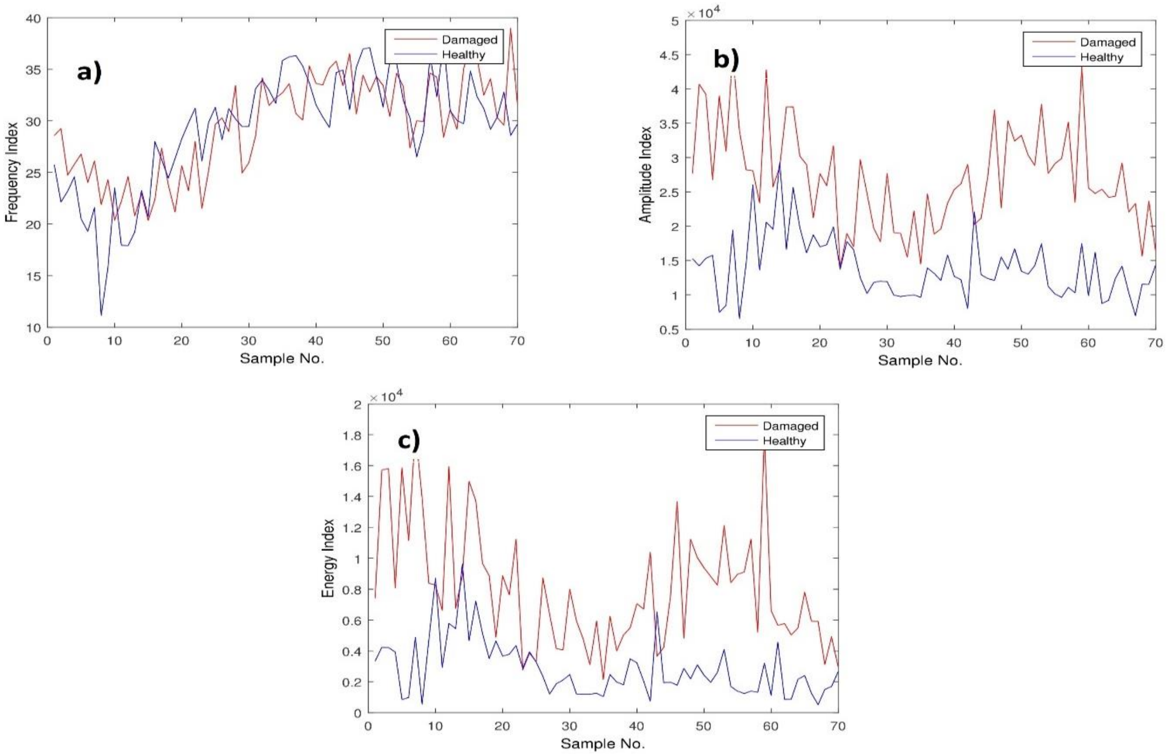

Fig. 11: Comparison of Damage Indexes for Healthy and Damaged Cases a) Frequency Index b) Amplitude Index (c) Energy Index

This sophisticated monitoring system is comprised of fourteen uniaxial accelerometers mounted on the deck as well as a biaxial accelerometer on the tower top, as shown in Fig. 6.

On January 17, 2008 data was collected in one-hour time intervals and repeated for 24 hours for the healthy state of the bridge. However, damages were identified during inspections in August 2008 including major cracks at both side spans and detachment of auxiliary pier. Therefore, data recorded on July 31, 2008 were reckoned as clear damage state of the bridge. For instance, Fig. 7 plots acceleration records of sensor 7 for both healthy and damaged cases.

5. Damage detection algorithm

5.1. Damage Index Selection

In this section the proposed damage detection technique is discussed in detail. First, a substructure technique is utilized by which the structure is divided into several substructures. The rationale is that for a large structure with many sensor outputs, it is difficult to identify all the structural parameters simultaneously. Reducing the size of the system not only prevents extensive computations, but also facilitates identification of local patterns. Fig. 3 displays three substructures on the bridge deck. Sensors 3, 7 and 11 are selected as the base sensors to monitor the deck and the supports condition. It is noteworthy to indicate that selection of the substructures has been based on structural mode shapes obtained from 3-D finite element model of the bridge (Li et al., 2014 [17]). For each substructure a base sensor is selected and the output of other sensors is not considered in the analysis (Fig. 6).

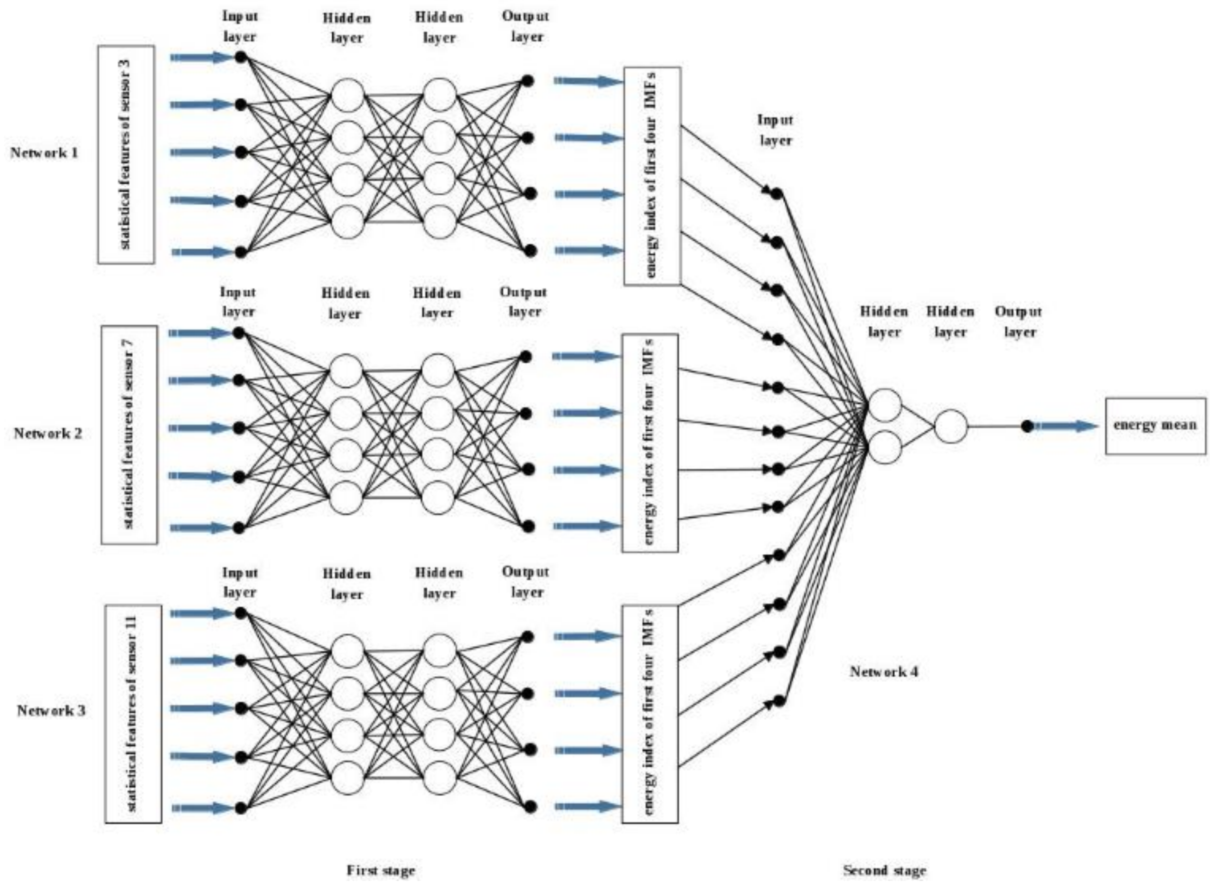

Fig. 12: Structure of the Neural Network Ensemble

For a reliable data analysis, signal length and sampling frequency must be large enough to reduce bias and random errors (Asmussen, 1997 [26]). Hilbert transform requires at least 5 samples per shortest period (Huang et al., 1998 [6]). On the other hand, over-sampling considerably enhances the accuracy of the analysis (Rilling and Flandrin, 2009 [27]; Li et al., 2010 [28]). In this study, sampling frequency of the sensors is 100 Hz. Hence, frequencies up to 50 Hz can be captured in accordance with Nyquist law. Moreover, Wenzel and Pichler (2005) [28] suggested a 5 min recording as the minimum length to find the structural parameters for common buildings. Also, Li et al. (2010) [29] estimated that 13.65 min time interval is adequate for PSD estimation of Yonghe bridge based on the Broch theorem (Broch, 2000 [30]). Accordingly, acceleration records are split to 15 min (900 s) time intervals. EMD is applied on the output records to extract the IMFs. Fig. 8 plots IMFs for the healthy state. Next, instantaneous frequencies and amplitudes are extracted using Hilbert transform.

Three signal features are first examined including frequency, amplitude and energy. For instance, Fig. 9 presents features of sensor 7 for the healthy case. One can observe large fluctuations in frequency values. To overcome this phenomenon, cumulative summation of absolute phase function is defined as frequency damage index (Fig. 10). The amplitude and energy damage indexes are also defined as

$$A_i = \int_0^T a_i \, dt \tag{27}$$

and

$$E_i = \int_0^T (IMF_i)^2 dt \tag{28}$$

Where subscript i denotes the IMF number.

A comparison of the aforementioned damage indexes is carried out in Fig. 11 for sensor 7 under healthy and damaged states. It is obvious that energy damage index performs better than the others in separating both cases. Thus, Energy index is employed for the following calculations. However, large variations exist due to environmental effects, specifically vehicle load vibrations.

5.2. Real-time damage detection technique

The procedure discussed above is computer-intensive and is not applicable for online monitoring. Besides, elaborate tracking of pattern changes in such a scattered data is complicated. Therefore, ANN is employed to diagnose the occurrence of damage. Since the damage is not known a-priori, training of the network is performed only for the healthy state. Thereby, when data for the damaged case is entered as the network input, outputs would differ which is accounted as a measure of damage. Initially, five traditional statistical features are used to characterize the time-domain information of the raw accelerometer data. These features are easily operated and need low computational time. Table 1 lists the definition of these features. These features are used as the network input.

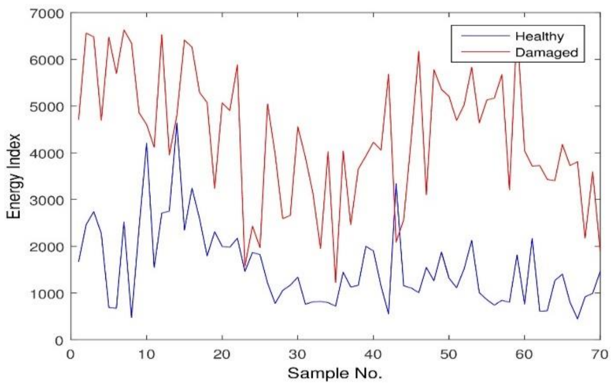

Fig. 13: Detection of Damage Using ANN

Since there is a disagreement among the accelerations of different sensors, using a single monolithic network can mix input data and destroy the damage patterns. Using an ensemble of independent networks helps to separate input spaces and reduces the generalization errors. Moreover, neural network ensemble has faster learning ability and need less computation efforts (Li et al., 2011 [31]). As a result, a two-stage network is utilized in this study. The first stage networks are designated for each sensor separately. They receive statistical features as input and send energy index of the first four IMFs as the output. Output of the first stage networks are set as the input for the second network. The final outcome of the network is the energy mean. First stage network has an input layer with five nodes, two hidden layers with four nodes and an output layer with four nodes, respectively. Hyperbolic tangent sigmoid transfer functions are assigned as activation functions. Training is made with back-propagation (BP) method. As aforementioned, training is carried out only by the healthy state data. Gradient descent algorithm is used to predict the weights and the biases of neurons. The second network contains twelve input nodes, two hidden layers and one output node. Fig. 12 shows the architecture of the neural network ensembles.

In general, the following steps outline the proposed real-time damage detection procedure:

1. Every 15 min (900 s), collect a sample of acceleration for each base sensor
2. Extract traditional statistical signal features
3. Use the trained ANN to calculate energy index
4. Compare the obtained energy index with healthy state energy indices

Fig. 13 shows the total energy index of damaged case in comparison with healthy state. In summary, ANN has proved its potential as a promising classifier to detect damage with an acceptable accuracy.

Table 1. Time-domain statistical features

root mean square	$\left(\frac{1}{N}\sum_{i=1}^{N} x_i^2\right)^{\frac{1}{2}}$
variance	$\frac{1}{N}\sum_{i=1}^{N}\left(x_i-\bar{x}\right)^2$
skewness	$\frac{1}{N}\sum_{i=1}^{N}\frac{\left(x_i-\bar{x}\right)^3}{\sigma^3}$
kurtosis	$\frac{1}{N}\sum_{i=1}^{N}\frac{\left(x_i-\bar{x}\right)^4}{\sigma^4}$
normalized sixth central moment	$\frac{1}{N}\sum_{i=1}^{N}\frac{\left(x_i-\bar{x}\right)^6}{\sigma^6}$

6. Conclusions

In this paper, a promising real-time damage detection technique is proposed using a combination of time-frequency signal processing and ensemble neural network. The former is the core of the solution to extract useful information from the data, and the latter is employed as a classifier. Based on the result the following conclusions can be drawn.

(i) Although several up-to-date instantaneous time-frequency techniques are proposed since the introduction of EMD, each have their own shortcomings. Therefore, still there is not a general time-frequency technique for the purpose of damage detection. Meanwhile, EMD is still a robust tool to decompose vibration signals of complex structures.

(ii) Although advanced signal processing techniques can be solely used for damage detection purpose, they do not fulfill expectations as an online damage detection tool. Using artificial intelligence in conjunction with signal processing helps to establish automatic algorithms that do not need expert intervention.

(iii) Environmental conditions, specifically variations of vehicle load, cause large dispersion in damage indices. In this paper, pattern recognition (e.g. ANN.) was utilized to track these variations. However, further research would be beneficial using stochastic [32-34], statistical [35,36], or probabilistic [37,38] approaches to handle such confounding fluctuations. Also, using inverse methods [39,40] may help to reduce the effect of environmental conditions and improve the accuracy of damage detection method.

Declaration of conflicting interests

On behalf of all authors, the corresponding author states that there is no conflict of interest

References

[1] Chen Z., Zhou X, Wang X, Dong L, Qian Y. Deployment of a smart structural health monitoring system for long-span arch bridges: A review and a case study. Sensors, 2017, 17(9): 2151.

[2] Hou Z, Hera, A, Noori M. Wavelet-Based Techniques for Structural Health Monitoring. In: Health Assessment of Engineered Structures, World Scientific Publishing, 2013: 179–201.

[3] Du R Engineering monitoring and diagnosis using wavelet transforms. In Computer-Aided Design, Engineering, and Manufacturing, CRC Press, 2019: 312-341.

[4] Yan R, Chen X, Mukhopadhyay S C. Structural Health Monitoring: An Advanced Signal Processing Perspective, Springer, 2017.

[5] Zhang R R, King R, Olson L, and Xu Y L. Dynamic response of the Trinity River Relief Bridge to controlled pile damage: modeling and experimental data analysis comparing Fourier and Hilbert–Huang techniques. Journal of Sound and Vibration, 2005, 285(4): 1049-1070.

[6] Huang N E, Shen Z, Long S R, Wu M C, Shih H H, Zheng Q, Liu, H H. The empirical mode decomposition and the Hilbert spectrum for nonlinear and non-stationary time series analysis. In Proceedings of the Royal Society of London A: Mathematical, Physical and Engineering Sciences, 1998, 454(1971):903-995.

[7] Liu J, Wang X, Yuan S, Li G. On Hilbert-Huang transform approach for structural health monitoring. Journal of Intelligent Material Systems and Structures, 2006, 17(8-9):721-728.

[8] Li H, Deng X, Dai H. Structural damage detection using the combination method of EMD and wavelet analysis. Mechanical Systems and Signal Processing, 2007, 21(1):298-306.

[9] Dong Y, Li Y, Lai M. Structural damage detection using empirical-mode decomposition and vector autoregressive moving average model. Soil Dynamics and Earthquake Engineering, 2010, 30(3): 133-145.

[10] Liu T Y, Chiang W L, Chen C W, Hsu W K, Lu L C, Chu T J. Identification and monitoring of bridge health from ambient vibration data. Journal of Vibration and Control, 2011, 17(4): 589-603.

[11] Roveri N, Carcaterra A. Damage detection in structures under traveling loads by Hilbert–Huang transform, Mechanical Systems and Signal Processing, 2012, 28:128-144.

[12] Kunwar A, Jha R, Whelan M, Janoyan K. Damage detection in an experimental bridge model using Hilbert–Huang transform of transient vibrations. Structural Control and Health Monitoring, 2013, 20(1):1-15.

[13] Hsu W K, Chiou D J, Chen C W, Liu M Y, Chiang W L, Huang P C. A case study of damage detection in four-bays steel structures using the HHT approach. Smart Structures and Systems, 2014, 14(4):595-615

[14] Ramezani S, Bahar O. EMD-based output-only identification of mode shapes of linear structures. Smart Structures and Systems, 2015, 16(5):919-35.

[15] Wang L, Chan T H. Review of vibration-based damage detection and condition assessment of bridge structures using structural health monitoring. QUT Conference Proceedings, 2009

[16] Chen B, Zhao S L, Li P Y. Application of Hilbert-Huang transform in structural health monitoring: a state-of-the-art review. Mathematical Problems in Engineering, 2014.

[17] Goyal D, Pabla B S. The vibration monitoring methods and signal processing techniques for structural health monitoring: A review. Archives of Computational Methods in Engineering, 2016, 23(4), 585-594.

[18] Smith J S. The local mean decomposition and its application to EEG perception data. Journal of the Royal Society Interface, 2005, 2(5): 443-454

[19] Feldman M. Time-varying vibration decomposition and analysis based on the Hilbert transform. Journal of Sound and Vibration, 2006, 295(3): 518-530

[20] Stepien, P. Sliding window empirical mode decomposition-its performance and quality. EPJ Nonlinear Biomedical Physics, 2014, 2(1): 14.

[21] Cheng J S, Zhang K, Yang Y, Yu D J. Comparison between the methods of local mean decomposition and empirical mode decomposition. Journal of vibration and shock, 2009, 28(5): 13-16.

[22] Huang Y, Yan C J, Xu Q. On the difference between empirical mode decomposition and Hilbert vibration decomposition for earthquake motion records. 15th World Conference on Earthquake Engineering, Lisboa, 2012.

[23] Henrici P. Applied and Computational Complex Analysis, Vol. 1: Power Series, Integration, Conformal Mapping, Location of Zeros. New York: Wiley, 1988.

[24] Li S, Li H, Liu Y, Lan C, Zhou W, Ou J. SMC structural health monitoring benchmark problem using monitored data from an actual cable- stayed bridge. Structural Control and Health Monitoring, 2014, 21(2), 156-172.

[25] Kaloop M. Structural health monitoring through dynamic and geometric characteristics of bridges extracted from GPS measurements. Doctoral dissertation. HIT. Harbin. China, 2010

[26] Asmussen, J C. Modal analysis based on the random decrement technique: application to civil engineering structures. Doctoral dissertation, unknown, 1997.

[27] Rilling G, Flandrin P. Sampling effects on the empirical mode decomposition. Advances in Adaptive Data Analysis, 2009, 1(01): 43-59.

[28] Wenzel H, Pichler D. Ambient vibration monitoring. John Wiley & Sons, 2005

[29] Li H, Li S, Ou J, Li H. Modal identification of bridges under varying environmental conditions: temperature and wind effects. Structural Control and Health Monitoring, 2010, 17(5): 495-512.

[30] Broch J T. Mechanical Vibration and Shock Measurements. Bruel & Kjaer: Naerum, Denmark, 2000.

[31] Li J, Dackermann U, Xu Y L, Samali B. Damage identification in civil engineering structures utilizing

PCA- compressed residual frequency response functions and neural network ensembles. Structural Control and Health Monitoring, 2011, 18(2):207-226.
[32] Skiadas C H. Recent advances in stochastic modeling and data analysis. World Scientific Publishing Company; 2007.
[33] Hamdia K M, Silani M, Zhuang X, He P, Rabczuk T. Stochastic analysis of the fracture toughness of polymeric nanoparticle composites using polynomial chaos expansions. International Journal of Fracture, 2017, 206(2): 215-227.
[34] Hamdia K M, Lahmer T, Nguyen-Thoi T, Rabczuk T. Predicting the fracture toughness of PNCs: A stochastic approach based on ANN and ANFIS. Computational Materials Science, 2015, 102: 304-313.
[35] Sprinthall RC, Fisk ST. Basic statistical analysis. Englewood Cliffs, NJ: Prentice Hall; 1990.
[36] Hamdia K M, Zhuang, X, He P, Rabczuk T. Fracture toughness of polymeric particle nanocomposites: evaluation of models performance using Bayesian method. Composites Science and Technology, 2016, 126: 122-129.
[37] Mitzenmacher M, Upfal E. Probability and computing: Randomization and probabilistic techniques in algorithms and data analysis. Cambridge university press, 2017.
[38] Vu-Bac N, Lahmer T, Zhuang X, Nguyen-Thoi T, Rabczuk T. A software framework for probabilistic sensitivity analysis for computationally expensive models. Advances in Engineering Software, 2016, 100: 19-31.
[39] Kirsch A. An introduction to the mathematical theory of inverse problems. Springer Science & Business Media, 2011.
[40] Vu-Bac N, Duong T X, Lahmer T, Zhuang X, Sauer R A, Park H S, Rabczuk T. (2018). A NURBS-based inverse analysis for reconstruction of nonlinear deformations of thin shell structures. Computer Methods in Applied Mechanics and Engineering, 331, 427-455.